WALAILAK JOURNAL
http://wjst.wu.ac.th Engineering and Physical Sciences

Effect of Mole Percentage of Crosslinker of Silver-poly(N-isopropylacrylamide-co-acrylic acid) Hybrid Microgels on Catalytic Reduction of Nitrobenzene

Zahoor H. FAROOQI[1,*], Shanza Rauf KHAN[2], Robina BEGUM[3], Tajamal HUSSAIN[1] and Nayab BATOOL[1]

[1]*Institute of Chemistry, University of the Punjab, New Campus, Lahore 54590, Pakistan*
[2]*Department of Chemistry, University of Agriculture, Faisalabad 38000, Pakistan*
[3]*Centre for Undergraduate Studies, University of the Punjab, New Campus, Lahore 54590, Pakistan*

([*]Corresponding author's e-mail: zhfarooqi@gmail.com)

Received: 19 December 2014, Revised: 26 January 2015, Accepted: 16 February 2015

Abstract

Poly(N-isopropylacrylamide-co-acrylic acid) microgels [P(NIPAM-co-AAc)] with 2, 4, 6 and 8 mole percentage of N,N-methylene-bis-acrylamide were used as micro-reactors for the fabrication of Ag nanoparticles using the *in situ* reduction method. The pure and hybrid microgels were characterized by Fourier transform infrared and Ultraviolet-Visible spectroscopies. Silver-poly(N-isopropylacrylamide-co-acrylic acid) hybrid microgels [Ag-P(NIPAM-co-AAc)] with different crosslinker contents were used as catalysts for reduction of nitrobenzene (NB) in aqueous medium in order to investigate the effect of crosslinker content on the value of apparent rate constant (k_{app}). 0.041, 0.146, 0.2388 and 0.255 min^{-1} were found as values of k_{app} for catalytic reduction of NB using hybrid microgels with 2, 4, 6 and 8 mole percentage of crosslinker, respectively. The effect of crosslinker feed content of hybrid microgels on catalytic activity for reduction of NB was compared to that of reduction of p-nitrophenol in aqueous medium.

Keywords: Microgels, crosslinker, nitrobenzene

Introduction

Metal nanoparticles are used enormously in antibacterial activities [1], cosmetics [2], sensing [3,4] and catalysis [5]. Noble metal nanoparticles are extensively used as catalysts in different oxidation and reduction reactions. Nanoparticles of silver (Ag) [6], gold [7], platinum [8] and palladium [9] have been found to be active catalysts for different reactions. Nanoparticles possess high surface-to-volume ratios, which is the reason why they are considered to be efficient catalysts in the present era [7,10-13]. Naked nanoparticles are rarely used in catalysis, because they coalesce rapidly. Coalescence forms big particles whose surface-to-volume ratios are smaller than that of nano-range particles. That is why nanoparticles are stabilized in some carriers and then used in catalytic applications. Responsive and non-responsive polymers have been reported to be carriers for catalytic applications of nanoparticles [14,15]. Responsive polymers swell and deswell in response to stimuli such as temperature, pH, and ionic strength [16-18]. Responsive microgels control the diffusion of reagents towards catalyst surfaces by swelling and deswelling in response to stimuli. Thus, catalysis can be tuned by various stimuli if nanoparticles are stabilized in responsive carriers [19,20]. Dendrimer [21], microgel [10], polyelectrolyte brush [22], core-shell [22], and yolk-shell [23] are different structures of responsive polymers in which nanoparticles have been stabilized. These structures have been also used as templates for the synthesis of nanoparticles. Among these structures, microgels have been found to be the best stabilizers and templates for the

synthesis of nanoparticles. Monodisperse nanoparticles are synthesized within microgel particles, because sieve size is uniform in them [24]. If nanoparticles are stabilized within microgels, they do not coalesce and leach after centrifugation or long term storage. Microgels can control the size and size distribution of *in situ* synthesized nanoparticles. Catalysis is a size-dependent application of nanoparticles. So, microgels are efficient for the catalytic application of stabilized nanoparticles.

The rate of catalysis can be tuned by parameters related to nanoparticles, microgels, and medium. Catalyst dosage and size, size distribution, and nature of the nanoparticles are nanoparticle-related parameters. The nature and feed of crosslinkers and monomers are microgel-related parameters. Temperature, pH, ionic strength, and solvent polarity are medium-related parameters. Many scientists have reported the effect of these parameters on catalytic reduction of p-nitrophenol (p-NP) [25-28]. We have also reported the effect of catalyst dosage [14], temperature [19], feed of monomers [29], and nature and size of nanoparticles [24,30] on the reduction of p-NP catalyzed by nanoparticle fabricated microgels. The effect of mole percentage of the crosslinker on the catalytic reduction of p-NP has been reported by our group previously [24]. In a previous report, it was observed that the value of k_{app} of catalytic reduction decreased with an increase in mole percentage of the crosslinker. Here, catalytic reduction of hydrophobic nitroarene (like nitrobenzene (NB)) is reported. In fact, this work is an extension of our previous report [24]. In our previous report, four samples of poly(N-isopropylacrylamide-co-acrylic acid) [P(NIPAM-co-AAc)] microgels with 2, 4, 6 and 8 mole percentage of crosslinker were synthesized. Then, these samples were used to synthesize Ag nanoparticles. Later, these microgels were used for catalytic reduction of p-NP (hydrophilic nitroarene). Here, catalytic reduction of NB (hydrophobic nitroarene) by using these microgels is reported. According to the best of our knowledge, the effect of the mole percentage of the crosslinker on the catalytic reduction of NB has not been reported in literature.

This article concerns the catalytic reduction of nitrobenzene by different Ag-P(NIPAM-co-AAc) hybrid microgels, and a comparison of that with p-NP using the same hybrid microgels.

Materials and methods

Nitrobenzene (NB), N-isopropylacrylamide (NIPAM), sodium dodecyl sulfate (SDS), acrylic acid (AAc), ammonium persulfate (APS) and N,N-methylene-bis-acrylamide (BIS) were obtained from Sigma-Aldrich USA. Sodium borohydride ($NaBH_4$) was purchased from Scharlau Company Germany. AAc was filtered through alumina for removal of inhibitors. All other remaining chemicals were used without any further purification. All solution preparations and synthesis were carried out using distilled water.

Synthesis of P(NIPAM-co-AAc) microgels and Ag-P(NIPAM-co-AAc) hybrid microgels

P(BIS-A), P(BIS-B), P(BIS-C), and P(BIS-D) microgel samples were synthesized by using 2, 4, 6 and 8 mole percentage of crosslinker, respectively, as reported previously [24].

Catalytic reduction of nitrobenzene

1.8 mL of 0.1 mM NB, 0.5 mL of 20 mM $NaBH_4$, and 0.2 mL of diluted dispersion of hybrid microgel were added into a cuvette. Then, spectra were scanned in the wavelength range of 190 to 400 nm on a UVD-3500 Laboomed Inc., spectrophotometer. Spectra were scanned after regular intervals of time until the reaction had been completed. Catalytic reduction of NB was studied by using the same amounts of NB, $NaBH_4$, and catalyst at 28±1 °C for every hybrid microgel sample (Ag-(PBIS-A), Ag-(PBIS-B), Ag-(PBIS-C), and Ag-(PBIS-D)).

Characterization

P(BIS-C) and Ag-(PBIS-C) samples were oven dried and their FTIR spectra were recorded on a Cary 630 FTIR spectrophotometer (Agilient Technology, United States of America). FTIR spectra were recorded in the range of 400 to 4000 cm^{-1}. UV-visible spectra of pure and hybrid microgels were recorded on a UVD-3500 (Laboomed Inc, United States of America). UV-visible spectra of diluted dispersions of pure and hybrid microgels were recorded in the range of 220 to 790 nm.

Results and discussion

FTIR spectra of P(NIPAM-co-AAc) microgels and Ag-P(NIPAM-co-AAc) hybrid microgels

FTIR spectra of P(BIS-C) and Ag-(PBIS-C) samples are shown in **Figure 1**. No absorption band around 1600 cm^{-1} is present in these spectra, which indicate that no unreacted monomer is present in the samples. The FTIR spectra of P(BIS-C) is similar to that of P(BIS-D), reported previously [24]. A comparison of absorption bands of different chemical bonds of P(BIS-C) and Ag-(PBIS-C) samples is given in **Table 1**. Two bands appeared in the 2800 - 3800 cm^{-1} range in the FTIR spectra of pure microgels. These 2 bands merged to give a broad band in the case of hybrid microgels. A lone pair of nitrogen of the –NH group and oxygen of the carboxyl group coordinated with Ag nanoparticles, so the vibration of –NH and –OH bands gets restricted, and the position of bands get shifted. This is the reason why 2 bands appeared in spectra of P(BIS-C) instead of a single band in this region. No new band is formed after the incorporation of Ag nanoparticles within microgels in the 400 - 4000 cm^{-1} range of FTIR spectra. The positions and intensities of bands are shifted only due to the coordination of different groups of polymers with nanoparticles. Dong *et al*. have also reported the shifting in bands after incorporation of Ag nanoparticles within P(NIPAM-co-AAc) microgels [31]. They explained it in terms of this donor-acceptor concept. Vimala *et al*. have also reported that position and intensity of bands were affected due to the loading of nanoparticles in hydrogels [32].

Table 1 Comparison of FTIR absorption bands of different functional groups of P(BIS-C) and Ag-(PBIS-C) samples.

Functional group	Chemical bond	Wavenumber (cm^{-1})	
		P(BIS-C)	Ag-(PBIS-C)
Carboxyl	C=O	1626	1648
Amide	C=O	1542	1560
Alkyl	CH_2 (bending)	1459	1460
Carboxyl	O-H (stretching)	2972	2970
Amine	N-H (stretching)	3281	3351

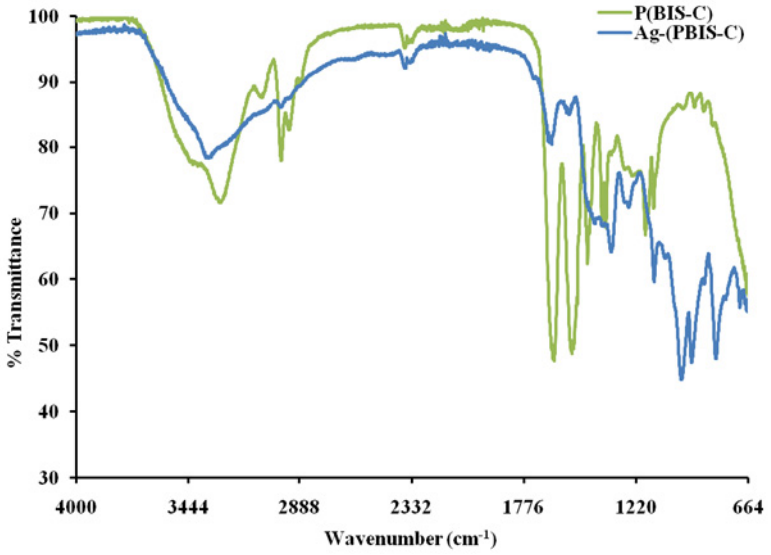

Figure 1 FTIR spectra of P(BIS-C) and Ag-(PBIS-C) samples.

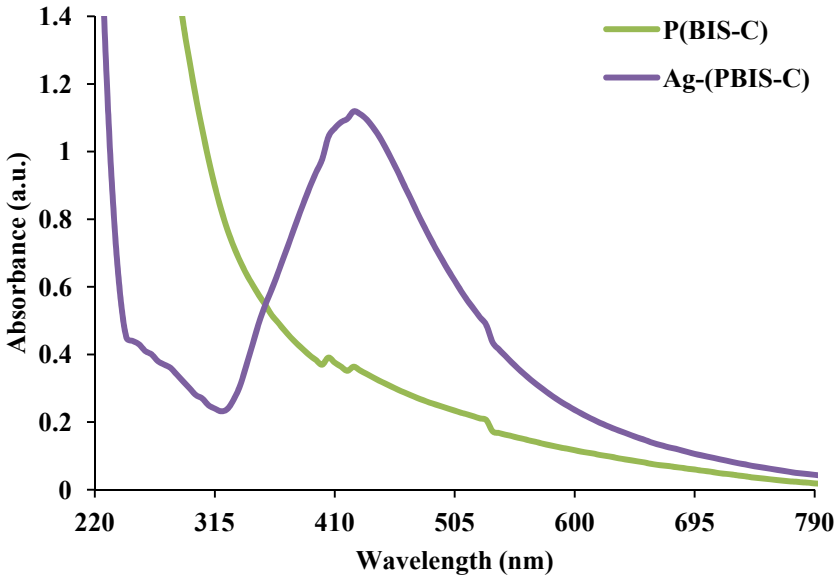

Figure 2 UV-Visible spectra of P(BIS-C) and Ag-(PBIS-C) samples.

UV-Visible spectra of P(NIPAM-co-AAc) microgels and Ag-P(NIPAM-co-AAc) hybrid microgels

The UV-Visible spectra of P(BIS-C) microgels and Ag-(PBIS-C) hybrid microgels are shown in **Figure 2**. The band around 425 nm in the spectra of hybrid microgel indicates the formation of Ag nanoparticles inside the microgel network. **Figure 2** also indicates that the Ag nanoparticles fabricated inside the microgel network are spherical in shape.

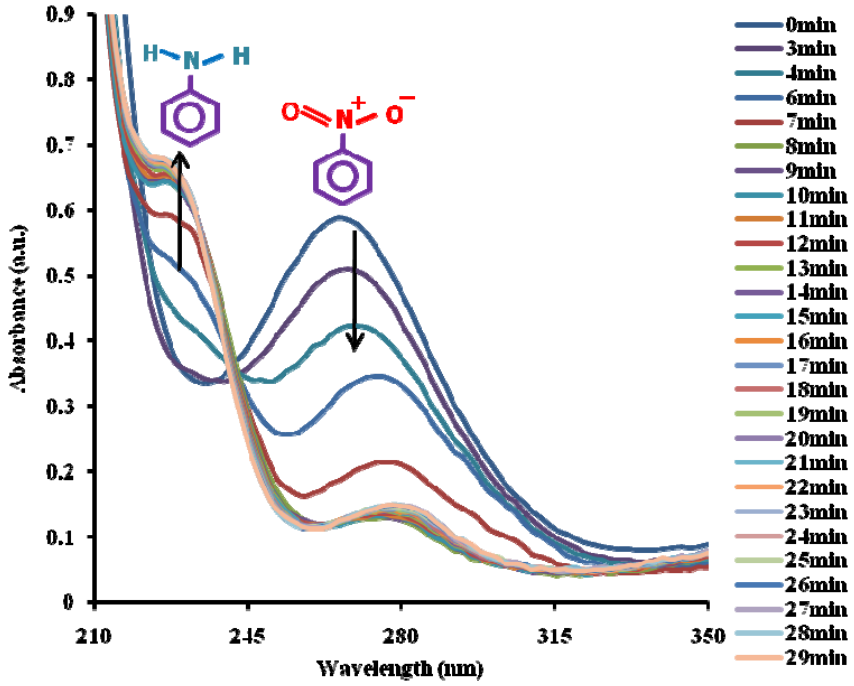

Figure 3 Time dependent UV spectra of reduction of NB in aqueous medium using Ag-(PBIS-C) hybrid microgels as catalysts (conditions: [NB] = 72 µM, Ag-(PBIS-C) = 0.2 mL, [$NaBH_4$] = 4 mM and temperature = 28±1 ºC).

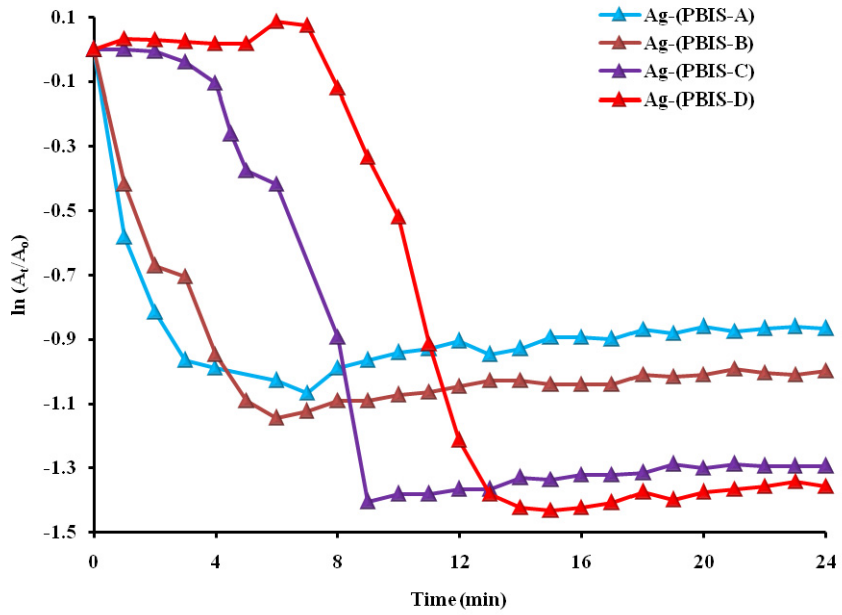

Figure 4 Plot of $\ln(A_t/A_o)$ as a function of time of catalytic reduction of NB in aqueous medium (conditions: [NB] = 72 µM, catalyst = 0.2 mL, [$NaBH_4$] = 4 mM and temperature = 28±1 °C).

Catalytic reduction of nitrobenzene

The catalytic reduction of NB into aniline in aqueous medium was monitored by UV spectrophotometry. Time-dependent UV spectra of the catalytic reduction of NB into aniline are shown in **Figure 3**. λ_{max} of NB is 268 nm, while λ_{max} of aniline is 231 nm [33]. Initially, NB is present in the reaction mixture, so λ_{max} at 268 nm appears initially. As the reaction progresses, NB is catalytically reduced into aniline. So, λ_{max} at 231 nm appears during the progress of reaction, but was not present initially, because aniline was not present in the reaction mixture initially. With the progress of reaction, concentration of NB decreases, and concentration of aniline increases at the same time. This is the reason why absorbance at 268 nm decreases and absorbance at 231 nm increases with the passage of time. So, λ_{max} of NB (268 nm) shows a hypochromic shift, while λ_{max} of aniline (231 nm) shows a hyperchromic shift with the progress of reaction. It was also observed that λ_{max} at 268 nm shifts to 270 nm during the progress of reaction. In fact, aniline slightly absorbs at 280 nm. This is why, as soon as aniline is formed in the reaction mixture, it shifts λ_{max} from 268 to 270 nm. The concentration of $NaBH_4$ was kept a hundred times greater than that of NB in the reaction mixture during all of the studies, so that the reaction followed the pseudo 1st order kinetic equation;

$$\ln \frac{A_t}{A_o} = k_{app} \times t \quad (1)$$

where A_o is absorbance at 0 min, and A_t is absorbance at time t. Slope of plot of $\ln(A_t/A_o)$ versus t is equal to k_{app}.

The catalytic reduction of NB was carried out in the presence of Ag-(PBIS-A), Ag-(PBIS-B), Ag-(PBIS-C), and Ag-(PBIS-D) hybrid microgels. A plot of $\ln(A_t/A_o)$ as a function of time for the reduction of NB catalyzed by different hybrid microgel samples was used for determination of k_{app} (**Figure 4**). **Figure 4** shows that the value of $\ln(A_t/A_o)$ did not change with time initially. This period at the start of the reaction in which the value of $\ln(A_t/A_o)$ did not change with time, is termed as the induction period. After the induction period, the value of $\ln(A_t/A_o)$ decreases with the passage of time, which indicates that the reaction is in progress. In the end, again, the value of $\ln(A_t/A_o)$ did not vary with time, which showed that the reaction had stopped. This showed that the maximum amount of NB was converted into aniline. The linear region of the plot of $\ln (A_t/A_o)$ versus time was used to calculate the value of k_{app}. The value of k_{app} of the catalytic reduction of NB in aqueous medium by different samples of hybrid microgels is plotted in **Figure 5**. The value of k_{app} of all plots is different from each other. This means that every hybrid microgel sample is catalyzing the reduction of NB at different rates. It has already been reported in our previous work that the size of the Ag nanoparticle is different in every hybrid microgel sample [24]. The surface area of nanoparticles is dependent upon their size. Catalysis is a surface related phenomenon, which is why the value of k_{app} was changed by changing the mole percentage of the crosslinker.

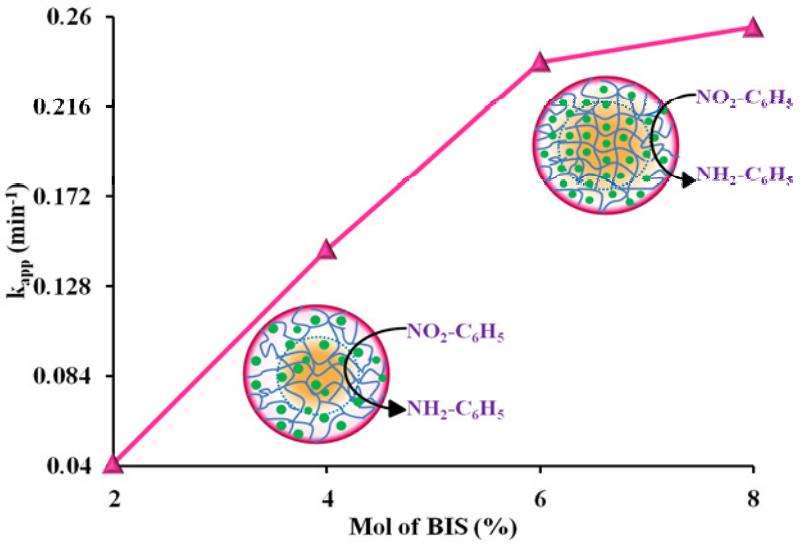

Figure 5 Effect of mole percentage of crosslinker on k_{app} of catalytic reduction of NB (conditions: [NB] = 72 µM, catalyst = 0.2 mL, [$NaBH_4$] = 4 mM and temperature = 28±1 °C).

Effect of mole percentage of crosslinker on apparent rate constant

The dependence of k_{app} of the catalytic reduction of NB on mole percentage of crosslinker is shown in **Figure 5**. It is shown from this plot that the value of k_{app} increases with an increase in mole percentage of crosslinker. This can be due to the combined effect of two reasons: (i) decrease in size of nanoparticle with increase in mole percentage of crosslinker, and (ii) increase in hydrophobic portion in network with increase in mole percentage of crosslinker. The surface area of nanoparticles increases with a decrease in size of nanoparticles. Therefore, the value of k_{app} increases with an increase in mole percentage of crosslinker. Crosslinker BIS and substrate NB are both hydrophobic. The hydrophobic portion in microgels increases with an increase in the content of crosslinker. As like attracts like, so hydrophobic NB get more strongly attracted towards microgels having a high mole percentage of crosslinker as compared towards microgels having a low mole percentage of crosslinker. These are two driving forces which cause an increase in the value of k_{app} with an increase in mole percentage of crosslinker.

The crosslinking density of microgels increases with an increase in mole percentage of crosslinker. With an increase in crosslinking density, sieve size decreases. So, the available space for the diffusion of reactants decreases with an increase in mole percentage of crosslinker. This causes a decrease in the value of k_{app}, with an increase in mole percentage of crosslinker. However, the results indicate that this effect is not dominant over the 2 aforementioned reasons. Thus, the value of k_{app} increases with an increase in mole percentage of crosslinker.

Figure 5 indicates that the value of k_{app} sharply increases with an increase in mole percentage of crosslinker from 2 to 6 mol %, but an increment in value of k_{app} is not sharply increased with an increase in mole percentage of crosslinker from 6 to 8 mol %. It has been reported that sieve size, crosslinking density, and the swelling ratio of microgels sharply varied when crosslinker content was low [11,34-36]. However, this variation is not so prominent when crosslinker content is high. The size of *in vivo* synthesized nanoparticles depends upon the structure of the microgel template. That is why the value of k_{app} sharply increases from 0.041 to 0.2388 min^{-1} by increasing crosslinker content from 2 to 6 mol %, and the value of k_{app} slightly increases from 0.2388 and 0.255 min^{-1} by increasing crosslinker content from 6 to 8 mol %.

Comparison of reduction of p-nitrophenol and nitrobenzene using same hybrid microgels as catalysts

In our previous report, Ag-(PBIS-A), Ag-(PBIS-B), Ag-(PBIS-C) and Ag-(PBIS-D) hybrid microgels were used as catalysts for the reduction of p-NP [24]. Here, we report the reduction of NB using these hybrid microgels as catalysts. For catalysis conditions, the concentration of substrate (p-NP/NB), catalyst, and $NaBH_4$ and temperature were kept the same for the catalytic reduction of both p-NP and NB. The values of k_{app} of catalytic reduction of p-NP were 0.568, 0.359, 0.320, and 0.313 min^{-1} for Ag-(PBIS-A), Ag-(PBIS-B), Ag-(PBIS-C), and Ag-(PBIS-D) hybrid microgels, respectively, while the values of k_{app} of catalytic reduction of NB were 0.041, 0.146, 0.2388, and 0.255 min^{-1} for Ag-(PBIS-A), Ag-(PBIS-B), Ag-(PBIS-C), and Ag-(PBIS-D) hybrid microgels, respectively. The value of k_{app} of catalytic reduction of p-NP is greater than that of NB for all hybrid microgel samples. Microgels are hydrophilic at 28±1 °C, as indicated in the previous report [24]. So, differentially crosslinked microgels favor catalysis of hydrophilic p-NP, as compared to that of hydrophobic NB. The value of k_{app} of the catalytic reduction of p-NP decreases with an increase in crosslinker feed content, while the value of k_{app} of the catalytic reduction of NB increases with an increase in crosslinker feed content. Crosslinking density of microgel increases with an increase in crosslinker mole percentage [24,37]. This means that highly crosslinked microgels possess a high feed of hydrophobic crosslinker [38]. So, high crosslinker feed containing microgels favor the catalytic reduction of NB as compared to that of p-NP. This is the reason why hydrophilic p-NP showed different trends in the value of k_{app} as compared to that shown by hydrophobic NB for the same hybrid microgel samples. This shows that substrate-catalyst compatibility also plays an important role in catalysis.

Conclusions

Ag-P(NIPAM-co-AAc) microgels were prepared with 2, 4, 6 and 8 mole percentage of crosslinker. P(NIPAM-co-AAc) microgels and Ag-P(NIPAM-co-AAc) hybrid microgels were characterized by Fourier transform infrared and UV-Visible spectroscopies. The application of Ag-P(NIPAM-co-AAc) hybrid microgels as catalysts for reduction of NB was studied by UV spectrophotometry. The value of k_{app} was found to be 0.041, 0.146, 0.2388, and 0.255 min^{-1} at 28±1 °C for hybrid microgel sample with 2, 4, 6, and 8 mole percentage of crosslinker, respectively. Here, a comparison of the effect of mole percentage of crosslinker on the value of k_{app} of catalytic reduction of NB and p-nitrophenol (p-NP) is given. It was observed that the value of k_{app} of catalytic reduction of NB increases with an increase in mole percentage of crosslinker, while that of p-NP decreases with an increase in mole percentage of crosslinker. This is due to the difference in nature of NB and p-NP. The value of k_{app} of the reduction of p-NP was found to be greater than that of NB, because microgels are hydrophilic at 28±1 °C, so they favor catalytic reduction of p-NP in comparison to that of NB.

Acknowledgements

This work was supported by the University of the Punjab, Lahore, Pakistan, under a university grant for the Fiscal Year 2015 - 2016.

References

[1] A Panacek, L Kvitek, R Prucek, M Kolar, R Vecerova, N Pizurova, VK Sharma, TJ Nevecna and R Zboril. Silver colloid nanoparticles: Synthesis, characterization, and their antibacterial activity. *J. Phys. Chem. B* 2006; **110**, 16248-53.

[2] S Kokura, O Handa, T Takagi, T Ishikawa, Y Naito and T Yoshikawa. Silver nanoparticles as a safe preservative for use in cosmetics. *Nanomed. Nanotechnol. Bio. Med.* 2010; **6**, 570-4.

[3] LS Lawson, JW Chan and T Huser. A highly sensitive nanoscale pH-sensor using Au nanoparticles linked by a multifunctional Raman-active reporter molecule. *Nanoscale* 2014; **6**, 7971-80.

[4] L Polavarapu, J Perez-Juste, QH Xu and LM Liz-Marzan. Optical sensing of biological, chemical and ionic species through aggregation of plasmonic nanoparticles. *J. Mater. Chem. C* 2014; **2**, 7460-76.

[5] J Santhanalakshmi and L Parimala. The copper nanoparticles catalysed reduction of substituted nitrobenzenes: Effect of nanoparticle stabilizers. *J. Nanopart. Res.* 2012; **14**, 1-14.
[6] N Pradhan, A Pal and T Pal. Silver nanoparticle catalyzed reduction of aromatic nitro compounds. *Colloids Surf. A* 2002; **196**, 247-57.
[7] S Carregal-Romero, J Pérez-Juste, P Hervés, LM Liz-Marzan and P Mulvaney. Colloidal gold-catalyzed reduction of ferrocyanate (III) by borohydride ions: A model system for redox catalysis. *Langmuir* 2009; **26**, 1271-7.
[8] J Pal, MK Deb, DK Deshmukh and BK Sen. Microwave-assisted synthesis of platinum nanoparticles and their catalytic degradation of methyl violet in aqueous solution. *Appl. Nanosci.* 2014; **4**, 61-5.
[9] F Tinnis, O Verho, KP Gustafson, CW Tai, JE Bäckvall and H Adolfsson. Efficient palladium-catalyzed aminocarbonylation of aryl iodides using palladium nanoparticles dispersed on siliceous mesocellular foam. *Chem. Eur. J.* 2014; **20**, 5885-9.
[10] G Agrawal, MP Schürings, P van Rijn and A Pich. Formation of catalytically active gold–polymer microgel hybrids via a controlled in situ reductive process. *J. Mater. Chem. A* 2013; **1**, 13244-51.
[11] S Carregal-Romero, NJ Buurma, J Perez-Juste, LM Liz-Marzan and P Herves. Catalysis by Au@pNIPAM nanocomposites: Effect of the cross-linking density. *Chem. Mater.* 2010; **22**, 3051-9.
[12] L Chen, J Hu, Z Qi, Y Fang and R Richards. Gold nanoparticles intercalated into the walls of mesoporous silica as a versatile redox catalyst. *Ind. Eng. Chem. Res.* 2011; **50**, 13642-9.
[13] Y Chen, C Wang, H Liu, J Qiu and X Bao. Ag/SiO_2: A novel catalyst with high activity and selectivity for hydrogenation of chloronitrobenzenes. *Chem. Commun.* 2005; **42**, 5298-300.
[14] SR Khan, ZH Farooqi, M Ajmal, M Siddiq and A Khan. Synthesis, characterization and silver nanoparticles fabrication in N-isopropylacrylamide-based polymer microgels for rapid degradation of p-nitrophenol. *J. Disp. Sci. Tech.* 2013; **34**, 1324-33.
[15] J Davarpanah and AR Kiasat. Catalytic application of silver nanoparticles immobilized to rice husk-SiO_2-aminopropylsilane composite as recyclable catalyst in the aqueous reduction of nitroarenes. *Catal. Commun.* 2013; **41**, 6-11.
[16] ZH Farooqi, A Khan and M Siddiq. Temperature-induced volume change and glucose sensitivity of poly [(N-isopropylacry-lamide)-co-acrylamide-co-(phenylboronic acid)] microgels. *Polym. Int.* 2011; **60**, 1481-6.
[17] ZH Farooqi, W Wu, S Zhou and M Siddiq. Engineering of phenylboronic acid based glucose-sensitive microgels with 4-vinylpyridine for working at physiological pH and temperature. *Macromol. Chem. Phys.* 2011; **212**, 1510-4.
[18] H Naeem, ZH Farooqi, LA Shah and M Siddiq. Synthesis and characterization of p (NIPAM-AA-AAm) microgels for tuning of optical properties of silver nanoparticles. *J. Polym. Res.* 2012; **19**, 1-10.
[19] M Ajmal, ZH Farooqi and M Siddiq. Silver nanoparticles containing hybrid polymer microgels with tunable surface plasmon resonance and catalytic activity. *Korean J. Chem. Eng.* 2013; **30**, 2030-6.
[20] R Contreras-Cáceres, J Pacifico, I Pastoriza-Santos, J Pérez-Juste, A Fernández-Barbero and LM Liz-Marzán. Au@pNIPAM thermosensitive nanostructures: Control over shell cross-linking, overall dimensions, and core growth. *Adv. Funct. Mater.* 2009; **19**, 3070-6.
[21] RM Crooks, M Zhao, L Sun, V Chechik and LK Yeung. Dendrimer-encapsulated metal nanoparticles: synthesis, characterization, and applications to catalysis. *Acc. Chem. Res.* 2001; **34**, 181-90.
[22] Y Mei, Y Lu, F Polzer, M Ballauff and M Drechsler. Catalytic activity of palladium nanoparticles encapsulated in spherical polyelectrolyte brushes and core-shell microgels. *Chem. Mater.* 2007; **19**, 1062-9.

[23] S Wu, J Dzubiella, J Kaiser, M Drechsler, X Guo, M Ballauff and Y Lu. Thermosensitive Au-PNIPA yolk–shell nanoparticles with tunable selectivity for catalysis. *Angew. Chem. Int. Ed.* 2012; **51**, 2229-33.
[24] ZH Farooqi, SR Khan, T Hussain, R Begum, K Ejaz, S Majeed, M Ajmal, F Kanwal and M Siddiq. Effect of crosslinker feed content on catalaytic activity of silver nanoparticles fabricated in multiresponsive microgels. *Korean J. Chem. Eng.* 2014; **31**, 1674-80.
[25] A Pich, A Karak, Y Lu, AK Ghosh and HJP Adler. Tuneable catalytic properties of hybrid microgels containing gold nanoparticles. *J. Nanosci. Nanotechnol.* 2006; **6**, 3763-9.
[26] S Praharaj, S Nath, SK Ghosh, S Kundu and T Pal. Immobilization and recovery of Au nanoparticles from anion exchange resin: Resin-bound nanoparticle matrix as a catalyst for the reduction of 4-nitrophenol. *Langmuir* 2004; **20**, 9889-92.
[27] N Sahiner, H Ozay, O Ozay and N Aktas. A soft hydrogel reactor for cobalt nanoparticle preparation and use in the reduction of nitrophenols. *Appl. Catal. B,* 2010; **101**, 137-43.
[28] N Sahiner, H Ozay, O Ozay and N Aktas. New catalytic route: Hydrogels as templates and reactors for *in situ* Ni nanoparticle synthesis and usage in the reduction of 2-and 4-nitrophenols. *Appl. Catal. A* 2010; **385**, 201-7.
[29] ZH Farooqi, SR Khan, R Begum, F Kanwal, A Sharif, E Ahmed, S Majeed, K Ijaz and A Ijaz. Effect of acrylic acid feed contents of microgels on catalytic activity of silver nanoparticles fabricated hybrid microgels. *Turkish J. Chem.* 2015; **39**, 96-107.
[30] ZH Farooqi, S Iqbal, SR Khan, F Kanwal and R Begum. Cobalt and nickel nanoparticles fabricated p (NIPAM-co-MAA) microgels for catalytic applications. *e-Polymers* 2014; **14**, 313-21.
[31] Y Dong, Y Ma, T Zhai, F Shen, Y Zeng, H Fu and J Yao. Silver nanoparticles stabilized by thermoresponsive microgel particles: Synthesis and evidence of an electron donor-acceptor effect. *Macromol. Rapid Commun.* 2007; **28**, 2339-45.
[32] K Vimala, KS Sivudu, YM Mohan, B Sreedhar and KM Raju. Controlled silver nanoparticles synthesis in semi-hydrogel networks of poly(acrylamide) and carbohydrates: A rational methodology for antibacterial application. *Carbohydr. Polym.* 2009; **75**, 463-71.
[33] T Zeng, XL Zhang, HY Niu, YR Ma, WH Li and YQ Cai. *In situ* growth of gold nanoparticles onto polydopamine-encapsulated magnetic microspheres for catalytic reduction of nitrobenzene. *Appl. Catal. B* 2013; **134**, 26-33.
[34] A Burmistrova, M Richter, C Uzum and R Klitzing. Effect of cross-linker density of P (NIPAM-co-AAc) microgels at solid surfaces on the swelling/shrinking behaviour and the Young's modulus. *Colloid. Polym. Sci.* 2011; **289**, 613-24.
[35] Y Dong, Y Ma, T Zhai, Y Zeng, H Fu and J Yao. Incorporation of gold Nanoparticles within thermoresponsive microgel particles: Effect of crosslinking density. *J. Nanosci. Nanotechnol.* 2008; **8**, 6283-9.
[36] K Gawlitza, ST Turner, F Polzer, S Wellert, M Karg, P Mulvaney and R von Klitzing. Interaction of gold nanoparticles with thermoresponsive microgels: Influence of the cross-linker density on optical properties. *Phys. Chem. Chem. Phys.* 2013; **15**, 15623-31.
[37] I Varga, T Gilányi, R Meszaros, G Filipcsei and M Zrínyi. Effect of cross-link density on the internal structure of poly (N-isopropylacrylamide) microgels. *J. Phys. Chem. B* 2001; **105**, 9071-6.
[38] H Senff and W Richtering. Influence of cross-link density on rheological properties of temperature-sensitive microgel suspensions. *Colloid. Polym. Sci.* 2000; **278**, 830-40.